TITLE: Thermohydraulic Analysis of Coolant Entry Patterns in a High-Temperature Pebble Bed

Reactor: Insights and Characterization

AUTHORS: Abel Gámez Rodríguez,Daniel Milian Pérez,Carlos Brayner De Oliveira Lira

Research Article

Thermohydraulic Analysis of Coolant Entry Patterns in a High-Temperature Pebble Bed Reactor: Insights and Characterization

[1*]A. Gámez Rodríguez (ID), [2]D. Milián Pérez (ID), [3]C. A. Brayner de Oliveira Lira (ID)

[1,2] Departamento de Energia Nuclear, Universidade Federal de Pernambuco (UFPE), Cidade Universitária, Avenida Professor Luiz Freire 1000, CEP: 50670-901, Recife, PE, Brasil.
[1,2,3] Centro Regional de Ciências Nucleares (CRCN-NE/CNEN), Cidade Universitária, Avenida Professor Luiz Freire 200, CEP: 50740-545, Recife, PE, Brasil.
E-mail: [1*]abel.rodriguez@ufpe.br

Abstract

Conducting three-dimensional thermohydraulic analysis of an entire nuclear reactor poses significant challenges due to the considerable geometric volume and complex internal structures involved. The top reflector is one of the internal structures found in high-temperature pebble bed Small Modular Reactors (SMR). This structure serves several critical functions, including neutron reflection, control and distribution of helium inlet into the core, neutron and thermal shielding, among others. In this kind of system, the detailed representation of the top reflector includes the representation of more than 460 channels of 2.5cm of diameter. Considering that the reactor has almost a ten of meters then dimension scales of various orders must be represented, which is a challenge. In this sense, a three-dimensional Computational Fluid Dynamics (CFD) thermohydraulic analysis of the entry pattern to the core of a High Temperature SMR using ANSYS CFX has been done. This study presents a comparison between five coolant entry patterns into the core. Initially, two prototype models of $460\times\varnothing2.5$cm, one with vertical channels and another with inclined channels, are modeled. Additionally, two prototype models of $20\times\varnothing12$cm of equivalent area, with vertical and inclined channels are also included. Finally, a simplified porous media model with the same equivalent area is considered. The thermohydraulic behavior of the coolant before and after passing through the top reflector was then analyzed for these five patterns. An analysis of fuel elements temperature in the core was conducted. It is important to highlight that this study is qualitative and has the goal of identifying and characterizing the impact that the coolant entry pattern into the reactor core has on the main thermohydraulic parameters in this region. The study exposes a strong correlation between the porous media model and all prototype models in terms of the maximum fuel temperature, average fuel temperature, and helium velocity. In this study, the potential applicability of the porous media models for an integral full-scale reactor simulation in the future was demonstrated. As a benefit, the porous media model reduces the mesh quantity compared to a prototypic model.

Keywords: CFD; HTR; porous media; top reflector detailed representation; thermohydraulic analysis.

1. Introduction

In the past decades, energy consumption has been increasing steadily around the world, and this trend is expected to continue in the future. Over the last decade, electricity demand rose by 25%, and it is estimated that between 30% and 43% annual growth in demand will occur up to 2030. To support this growth, it is estimated that the global energy supply should grow between 1.0% and 1.3% per year [1], [2]. The nuclear industry, with more than six decades of developing and improving technologies, has proven to be an outstanding potential solution to meet the growing energy demand safely and economically. The capabilities of the nuclear industry are being reinforced by the innovations planned for the generation IV (Gen-IV) reactor technologies, which offer significant improvements compared to current nuclear technologies in terms of closing the fuel cycle, waste minimization and enhanced resource use, inherent safety, economics, and proliferation resistance and security [1]. In recent years, there has also been a growing interest in merging the Gen-IV and the small modular reactor technologies. At the moment, all the Gen-IV technologies are in the research and development stages. All the research and development activities related with those advanced systems are being followed closely by the Generation IV International Forum (GIF).

In the two decades that have passed, since the establishment of the GIF in 2000, various Gen-IV reactor technologies have been evaluated. The Very-High-Temperature Reactor (VHTR) has been identified as one of the most promising reactor concepts for the next generation of nuclear reactors by the International Atomic Energy Agency (IAEA) [3]–[6]. It utilizes ceramic fuel, graphite as a moderator, and helium gas as a coolant. The VHTR builds on the experience gained from a group of experimental and commercial High-Temperature Gas-Cooled Reactors (HTGR) that were built and operated during the latter half of

the 20th century, along with two ongoing projects. The former includes Dragon in the United Kingdom, Peach Bottom and Fort St. Vrain in the United States, and AVR (*German*: Arbeitsgemeinschaft Versuchsreaktor) and the Thorium High-Temperature Reactor (THTR) in Germany. The latter are the High-Temperature Test Reactor (HTTR) in Japan and the HTR-10 in China, which became operational in early 2000, respectively. These experiences and advancements have led to the development of the VHTR, which holds great promise for the future of nuclear energy [7].

Making predictions about the thermohydraulic behavior of High Temperature Reactors is a crucial contribution to advancing VHTR technology. Despite the advances made in the development and study of VHTRs, there are still some key challenges that need to be addressed before the commercial deployment of this technology can be realized. These challenges include improving the nuclear safety characteristics, addressing the cost-effectiveness of the technology, developing appropriate fuel and waste management strategies, and addressing issues related to the supply chain and infrastructure. Ongoing research, development, and demonstration of important systems design and analysis are needed to overcome these challenges and ensure the successful implementation of VHTR technology [5], [6], [8].

The use of digital engineering, integrated numerical tools and high-level software for the simulation of these systems constitute an effective initial alternative to scale model proof. Reducing, time cost, the number of new experimental facilities and tests required during the experimental testing phase [9], [10]. Indeed, one of the current challenges in the engineering community is to obtain fast and realistic results of different configurations of diverse prototypes using experimentation in controlled conditions. This challenge almost always is extremely difficult and expensive. Mainly including expensive measurement techniques, and advanced sensors. Sometimes, involving measurement of inaccessible volume, or small for intrusive/non-intrusive measurement. And more difficult considering hostile environments such as the high temperature, chemical contaminants, radioactive, etc. In this sense, the Computational Fluid Dynamics (CFD) appears to be a logical way to complement experimentation [11]. On the other hand, to validate CFD models accurately simulating the thermohydraulic processes within the reactors, experimental data is essential.

In this sense, the experimental reactor HTR-10 was selected as a reference reactor of high temperature pebble bed gas-cooled reactor by the IAEA to study the performance of some technology components under different conditions [6]. The HTR-10 stands as one of the SMRs utilizing this technology and is currently operational [5]. Making predictions about the thermohydraulic behavior of High Temperature Reactors (HTR) is a crucial contribution to advancing VHTR technology. The computational prediction of the thermohydraulic behavior of this reactor involves different physic-neutronic approach and detailed structural information. Multiscale approach and multiphysics coupled techniques are others of the challenges in the simulation of real situations [12]. Thus, performing a comprehensive three-dimensional thermohydraulic analysis of an entire nuclear reactor poses a significant challenge due to the vast geometric volume and intricate structures involved [13].

However, the correct prediction of the coolant behavior inside the internal structures and the impact of different configurations of these internal structures in the reactor core continue to be challenges to the international research community. Optimized design and the safety performance of the internal structures continue to be the stay of the art. The top reflector is one of the internal structures found in high-temperature pebble bed SMRs. This structure serves several critical functions, including neutron reflection, control and distribution of helium inlet into the core, neutron and thermal shielding, among others.

To the best of the authors' knowledge, no detailed descriptions of the internals of the top reflector are available in the literature. According to [14], [15], the bricks below the cold plenum have 460 machined holes with 2.5cm of diameter through which cold helium flows down from the cold gas chamber into the reactor core. Nothing was indicated about the distribution or the inclination of these holes in the reflector bricks. Knowing only the number of channels and their diameter, it is impossible to adequately represent that section of the reactor geometry. That is why, over the years several articles have been made around the HTR-10, and in all of them, it has been modeled using different approximations of the internal construction details of the top reflector.

In [16] was studied one postulate design accident applying 3D modelling. In that study, the investigation centered on the hydrogen generation resulting from the reaction between graphite and water subsequent to a steam generator tube rupture. The study did not represent the characteristic coolant flow pattern within the core region but assumed a homogeneous vertical flow as the coolant inlet condition. Additionally, in [17] was analyzed the air ingress occurred after the Loss-of-Coolant Accident (LOCA) with double-ended rupture of the gas duct tube in the same pebble-bed reactor. In that paper were represented a few verticals channels to simulate the path of the coolant through the top reflector as a connection between the cold plenum and the reactor core. Other studies using the coarse mesh-based system-level codes have been used for HTGR safety analysis according to [13]. Other 2D axisymmetric thermohydraulic codes were used to analyze steady state and transient behavior of the HTR-10 using the porous media approximation according to [14]. Another example was [12], where 20 inclined channels of diameter 12 centimeters were utilized, employing an equivalent area simplification.

As observed, all these studies utilized varying approximations to represent the coolant's entry pattern into the core. However, no experimental studies or simulation investigations were found that address the potential impact of the coolant entry pattern into the core of this type of reactors. This gap in the existing literature underscores the originality and significance of the present study, which aims to fill this knowledge void and provide valuable insights into the thermohydraulic behavior of the reactor core under different coolant entry scenarios.

In this sense, the goal of this paper is to identify and characterize the impact in the main thermohydraulic parameters due to the approximation used to represent the coolant entry pattern into the core of the pebble bed high temperature reactor prototypes. In this paper, the three-dimensional CFD thermohydraulic analysis of the entry pattern to the core of the HTR-10 using ANSYS CFX has been done. This study presents a comparison between different patterns of the entry of coolant into the core: two
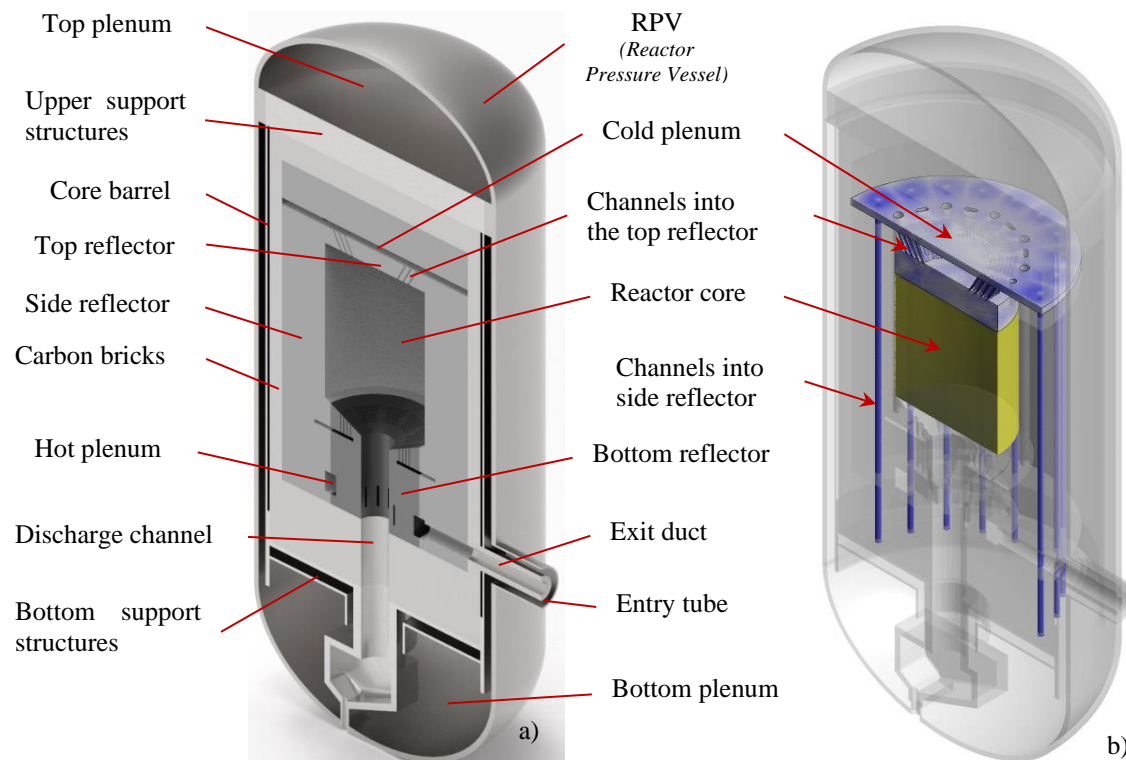
Figure 1. The main CAD geometries of the reactor structures a); blue and yellow the regions simulated in this study b).

prototype models of 460x⌀2.5cm distributed vertical and inclined channels, and two models of 20x⌀12cm of equivalent area vertical and inclined channels, also a simplified porous media model.

A thermohydraulic analysis of the coolant was conducted after examining five different representations of the coolant crossing through the top reflector. An analysis of the impact of the different ways of representing the coolant entrance to the reactor core on the temperature of the fuel elements was also carried out.

2. Methodology and Mathematical Model

To simulate the thermohydraulic characteristics of the coolant within the specified region inside the HTR-10 reactor, we used the model proposed by [12] as a reference. Geometric representation of the reactor structures was achieved using 3D CAD software such as Dassault Systèmes SOLIDWORKS and ANSYS SpaceClaim. These were used to represent the regions defined as coolant (fluid domains) and a mixture region of fuel and helium (porous domains). All of these regions were defined by the void space inside the specific structural components. The level of detail of the represented geometric models was defined based on the required precision, the scale resolved in the study and the available computational resources. The required precision in our geometric models was determined based on the specific parameters and phenomena under investigation. In particular, we considered factors such as the size of the channels in the top reflector, the variations of the coolant flow, and the thermal characteristics within the pebble-bed reactor. It's worth noting that all these geometric parameters were defined by IAEA [14], except for the distribution of the 460 channels of coolant in the top reflector. The lack of detailed description in [14] regarding the distribution of the 460 channels of coolant in the top reflector serves as a key motivation for conducting this study. In this sense, a three-

dimensional full-scale representation was created for the following regions: the vertical channels into the side reflector, the cold plenum, the prototypes pattern to represent the channels into the top reflector, the cavity before the pebble-bed in the reactor core, and the pebble-bed itself, as shown in Figure 1.

It is crucial to emphasize that this study is qualitative and aims to identify and characterize the impact of the coolant entry pattern into the reactor core on the main thermohydraulic parameters in this region. Following this premise, only the regions of coolant circulation closest to the study area were represented, focusing exclusively on studying the impact of different flow patterns at the core inlet. Therefore, thermal exchanges between the coolant and any structural element before entering the reactor core have been neglected. In all of the cases, no contact between the coolant and the structural elements will be considered, which will lead to ideal adiabatic conditions in these regions. This consideration will imply that the estimated temperatures are much more conservative than the real operating temperatures. For this, ANSYS CFX 19.0 software was employed [12], [18], [19]. Energy transport equation was used to consider the heat transfer between the fuel surface temperature and the coolant. The porous media approach was adopted to simulate the closely packed pebbles in the core.

In the present simulation, a non-uniform distribution of the packed pebble porosity was assumed to simulate wall effects. The base description of the integral 3D thermohydraulic simulation of the steady state of this reactor was proposed by [12].

2.1 Patterns of the Entry of Coolant into the Reactor Core

Figure 2 shows the coolant pattern of the simulated region inside the reactor and the patterns of coolant entry into the reactor core. Initially, two prototype models consisting of
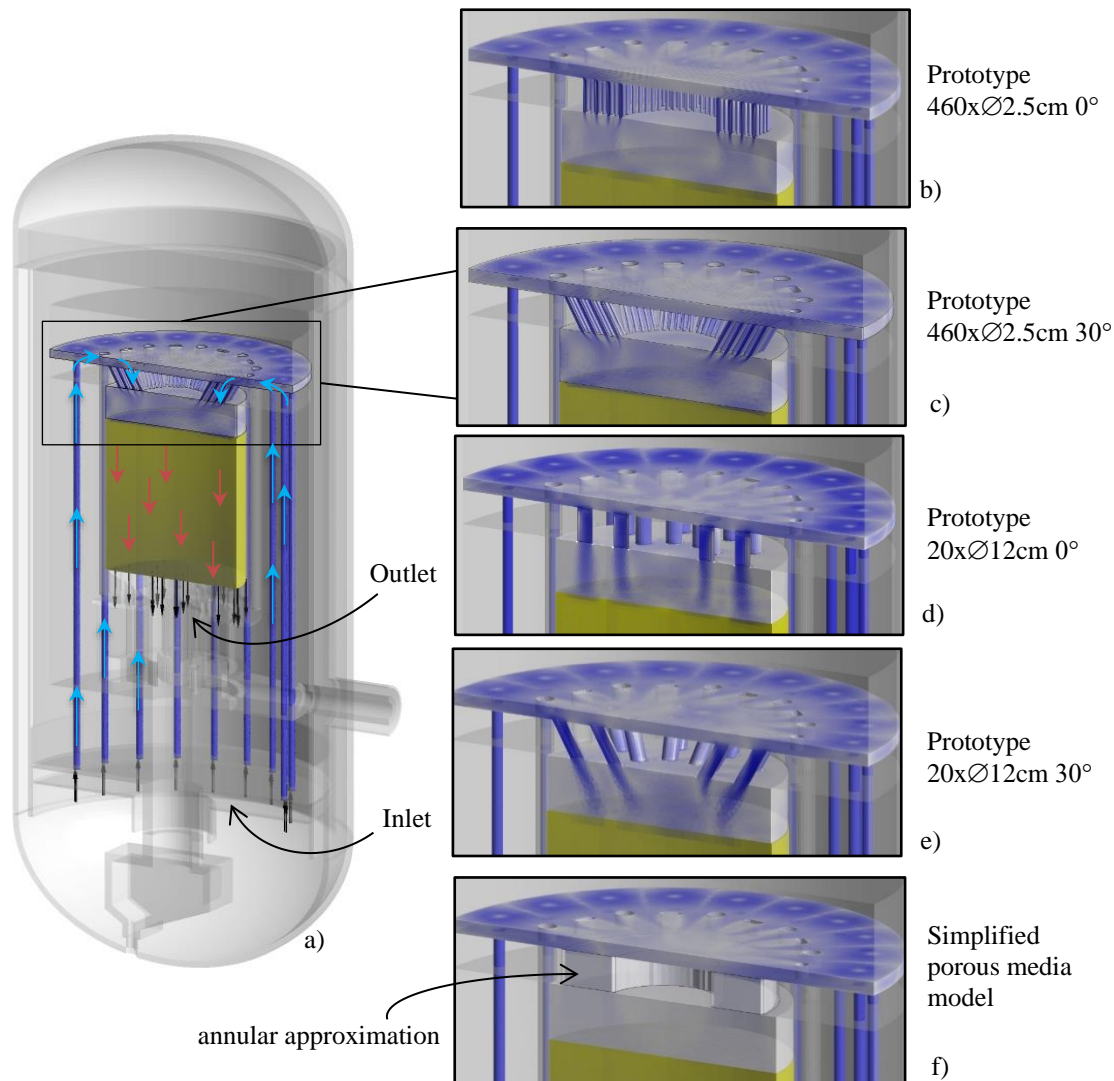
Figure 2. Schematic fluid flow of the simulated region inside the reactor a), and the coolant flow representation from the five analyzed patterns b) to f).

460 small channels, each with a diameter of 2.5cm, are distributed around the top reflector, as outlined in [15]. These channels are depicted either vertically (Figure 2 b) or at a 30-degree angle (Figure 2 c). Also, two models of 20 channels with 12cm of diameter representing the equivalent area used by [12]. Likewise, the larger channels were also represented vertically (Figure 2 d) or at a 30-degree angle, as illustrated in Figure 2 e). Finally, a simplified vertical porous media model as shown in (Figure 2 f). The five models have the same transversal equivalent area. However, their primary distinction lies in the pattern of turbulent flow generated within the top cavity of the core.

Based on these patterns, an analysis of the thermohydraulic behavior of the coolant before and after crossing the top reflector was carried out. Also, the impact of the use of these patterns in the prediction of average thermohydraulic parameters in the pebble-bed hot core zone was studied.

2.2 The Domain of Numerical Models and Boundary Conditions

The methodology employed in this article has been previously discussed in [12]. Specifically, in this paper, an equivalent mass flow rate to the helium flow under normal operating conditions of the HTR-10 reactor will be considered as the inlet condition. This flow is defined in the vertical direction in the cooling pipes of the side reflector, as shown in Figure 2. As the outlet condition, the transverse region of the reactor core just before the conical contraction has been selected, as illustrated in Figure 2.

A symmetry condition was placed on an axial plane, both in the region occupied by the entry patterns, the upper plenum, and the interior region of the reactor core, similar to what is shown in the methodology [12]. Also, the adiabatic no-slip wall option was considered for all other surfaces of the analyzed models. This last selection, will induce elevated temperature values throughout the fuel element bed region, as there will be no thermal exchange with the structural elements and reflectors through which helium flows. Nevertheless, this will illustrate the differences between the studied models without the influence of thermal exchange with these structures. This allows us to evaluate the impact of representing the coolant entry pattern into the reactor core.

2.3 Mathematical Models

In order to computationally simulate the flow of helium and the region occupied by the fuel elements, a comprehensive mathematical model was employed. This model encompasses the fundamental equations governing fluid dynamics, including the continuity equation, momentum conservation equation, and energy conservation equation. Additionally, the model incorporates the state

equation and two supplementary equations for the turbulence model. In general, ANSYS CFX uses a coupled solver, which solves the hydrodynamic equations (for u, v, w, p) as a single system. This solution approach involves a fully implicit discretization of the equations at any given time step. For steady-state problems, the time-step acts as an 'acceleration parameter', guiding the approximate solutions toward a physically based steady-state solution. This reduces the number of iterations required for convergence to steady-state or to calculate the solution for each time step in a time-dependent analysis [20].

Therefore, the simulation was executed using ANSYS's suite of codes: CFX-Pre for model setup, CFX-Solver for solving the equations, and CFD-POST for post-processing. The ANSYS CFX solver is specifically designed to calculate the unsteady Reynolds-averaged Navier-Stokes equations in their conservation form [20].

2.3.1 The Continuity Equation

The continuity equation or the mass conservation equation is shown below:

$$\frac{\partial \rho}{\partial t} + \nabla \cdot (\rho \boldsymbol{U}) = 0 \tag{1}$$

where t represents the time, ρ is the fluid density, and U is the velocity field.

The principle of momentum conservation states that the total forces exerted on a fluid element will consistently equal the change in momentum of that element. When accounting for both surface forces and forces acting within the body of an infinitesimal volume element, a simplified representation of the momentum conservation law can be formulated as follows:

$$\frac{\partial (\rho \boldsymbol{U})}{\partial t} = \nabla \cdot (\rho \boldsymbol{U} \otimes \boldsymbol{U}) = -\nabla \mathrm{p} + \nabla \cdot \boldsymbol{\tau} + S_M \tag{2}$$

In this equation the parameter $\boldsymbol{\tau} = \mu \left[(\nabla \boldsymbol{U} + \nabla \boldsymbol{U}^T) - \frac{2}{3} \delta \nabla \cdot \boldsymbol{U} \right]$ is the stress tensor; p represents the pressure field, S_M is a source term that considers other effects [20].

2.3.2 The Thermal Energy Equation

Particularly, in fluid domains, the conservation of energy equation elucidates the mechanisms of heat transport attributed to fluid motion, conduction, and volumetric heat sources [20].

The most robust formulation for the energy equation within ANSYS CFX is the Total Energy formulation, which encompasses the total enthalpy. An alternative expression of the energy equation, which is suitable for low-speed flows from static enthalpy is the thermal energy equation:

$$\frac{\partial (\rho h)}{\partial t} + \nabla \cdot (\rho \boldsymbol{U} h) = \nabla \cdot (\lambda \nabla T) + \boldsymbol{\tau} : \nabla \boldsymbol{U} + S_E \tag{3}$$

In this formulation, the term $\boldsymbol{\tau} : \nabla \boldsymbol{U}$ represents the dissipation function representing the work done against viscous forces (viscous dissipation). Here, h denotes the enthalpy and λ represents the thermal conductivity. The terms S_E symbolize a heat source considered as a contributory factor to decay heat and fission power.

For the simulation of heat generation, a system of cylindrical and annular regions was employed, releasing heat from nuclear fission and radioactive decay. This approach, discussed previously in [12], was initially proposed by the IAEA in [14], and serves as a reference for the reactor power distribution under normal operation.

2.3.3 Equation of State

The transport equations described above must be complemented with constitutive equations of state for density and enthalpy to form a closed system. In the most general case, these states have the following form:

$$\rho = \rho(p, T) \tag{4}$$

$$dh = \frac{\partial h}{\partial T} |_p \, dT + \frac{\partial h}{\partial p} |_T \, dp = C_p dT + \frac{\partial h}{\partial p} |_T \, dp \tag{5}$$

$$C_p = C_p(p, T) \tag{6}$$

Together, all equations commented so far are solved in the CFD code simultaneously. Obtaining a detailed description at any point or region of interest.

2.4 Turbulence

One of the most important phenomena described by fluid dynamics is the phenomenon of turbulence. In this phenomenon, fluid movement is characterized by random or chaotic fluctuations in the form of swirls, vortices, etc. These fluctuations can be caused by surface imperfections and/or obstacles in the free flow of fluid and both small and large scales.

The extended Navier-Stokes equations are capable of representing both laminar and turbulent flows without requiring additional information, but this comes at the expense of high computational costs that can often be prohibitive. Furthermore, for flows with specific Reynolds numbers, a wide range of scale representations is required, some of which are significantly smaller than the finite volume mesh that can be reasonably utilized in numerical analysis. Direct Numerical Simulation (DNS) of these flows would require computational resources that are many orders of magnitude greater than those currently available. For that, turbulence models have been specifically developed to account for the effects of turbulence without recourse to a prohibitively fine mesh [20]. In general, turbulence models seek to modify the original Navier-Stokes equations, which are unstable, by introducing average and fluctuating quantities. These modifications give rise to the Reynolds Averaged Navier-Stokes (RANS) equations.

A group of turbulence models, headed by the RANS models, are widely used to represent most practical engineering problems. In this group, are used statistical turbulence models based on the Reynolds time mean equations, knowing only the effects of turbulence on the mean flow.

On the other hand, the preceding investigation [12], [14] showcased the application of the κ-ε turbulence model. In them, an outstanding correlation was established between simulating the steady state at maximum power for the HTR-10 reactor and experimental data, all achieved at a minimal computational cost. Hence, in this current study, we opt for the turbulence model grounded in the Reynolds equations

(temporal mean - RANS) with the two-equation turbulence model: standard κ-ε.

2.5 Pebble Bed Porous Media Simulation Approach

In this work, it was considered a porous media in the approximate region of the reactor core occupied by fuel pebbles which are cooled by the helium flow. In this region was used the Full Porous formulation that solve a finite temperature difference between the fluid phase and the solid phase. Full Porous is a non-thermal equilibrium model when the separate energy equations for each phase within the domain are computed and the temperature field is assumed as average temperatures.

All heat transfer effects between fuel elements and helium within the pebble bed were considered. This was accomplished through the implementation of the overall heat transfer coefficient in the reactor core region [12]. The coefficient used was proposed by the KTA after thorough experimental studies, considering conduction, convection, and thermal radiation [21]. The approach to representing the heat transfer within the reactor core using the porous media was analyzed in more detail in [12]. This detailed analysis supports the robustness and validity of the chosen methodology in capturing the essential aspects of heat transfer phenomena in the reactor core.

In [12], are discussed in detail the selection of the mathematical model to estimate the temperature in the center of the fuel elements, the isotropic porous media pressure losses, thermal and materials properties correlations, and others modeling related topics. The variation with pressure and temperature of helium properties, such as thermal conductivity, dynamic viscosity, and density, were implemented according to [22].

On the other hand, the reactor core is designed for a thermal power of 10 MW, with a gas pressure and mass flow in the primary circuit of 3.0 MPa and 4.32 kg/s, respectively in normal operation. It has a gas outlet temperature of 700 °C and a gas inlet temperature of 250 °C [23]. However, it is known that part of the helium coolant bypasses the main flow path (leaks) due to clearances among structural elements and graphite blocks. Conservatively, it is assumed that this bypassing part of the helium flows directly from cold helium entry to hot helium exit, making it non-effective for core cooling. The following flow rates and leakages are considered:

- The Rated Coolant Flow Rate (RCFR) is 4.32 kg/s.
- 1% of the RCFR passes through the fuel discharging tube to cool fuel elements in the tube.
- 2% of the RCFR flows through the control rod channels to cool the control rods.
- The maximum bypassing leakage among bottom graphite blocks is assumed to be 10% of RCFR.

Therefore, 87% of the RCFR flows through the pebble bed zone, effectively cooling fuel elements in the core. These approximations were widely used in [14] and more recently in [12].

2.6 Pressure Drop Through the Top Reflector Considering a Simplified Porous Media Model

As previously stated, in addition to the reactor core, the patterns of the entry of coolant into the reactor core were also represented using a vertical porous media simplification. As shown in Figure 2 f). For that, the simplified vertical porous media model represents the joint region between the cold helium plenum and the top cavity of the core region. In this approximation, was considered that the 460x$\varnothing$2.5cm straight coolant channels as the vertical direction inside the top reflector bricks as a simple annular region of 160cmx78cmx25cm. Was imposed in this annular region a bulk porosity equivalent to the relation between the volume occupied by the 460x$\varnothing$2.5cm channels and the volume of an annular region as shown in Figure 2. Also, it was considered the permeability and inertial resistance factor in the vertical direction (streamwise direction) only. The resistance in the transverse direction was be assumed substantially highest to prevent unphysical horizontal cross flow. This effect was implemented using the Directional Loss Model, allowed in Ansys CFX [18]. For this, the resistance along the flow direction from Darcy-Weisbach model was used.

To estimate the Reynold number that characterize the movement of coolant through the 460x$\varnothing$2.5cm channels ($Re_{2.5cm}$) was used the following consideration:

- Only the 87% of the reactor mass flow rate cross the top reflector through the 460 channels of $\varnothing$2.5cm to the reactor core as was indicated in the section 2.5 and used in [14].
- The same distribution of the mass flow rate crossing all the channels.
- The coolant crosses the channels to 250 °C, then

$$Re_{2.5cm} = \frac{\dot{m}_{2.5cm} * d_{2.5cm}}{A_{2.5cm} * \mu} = 14\ 152 \tag{7}$$

Where:
$\dot{m}_{2.5cm}$: mass flow rate crossing an individual channel.
$\dot{m}_{2.5cm} \approx 8.17E - 03\ [kg\ s^{-1}]$
$d_{2.5cm}$: diameter of a channel, $\varnothing$2,5cm.
$A_{2.5cm}$: Cross section area of a channel.
μ: Dynamic viscosity of the coolant corresponding to 250 °C.

For the solution of the corresponding pressure loss due to coolant through the top reflector for the simplified vertical porous media model, was used the universal formula proposed by Darcy-Weisbach [24]. The Eq. (8) describes the pressure loss, denoted as ΔP, resulting from inertial effects in a cylindrical pipe with a uniform diameter.

$$\frac{\Delta P}{L} = f \frac{\rho}{2} \frac{\bar{V}^2}{D} \tag{8}$$

In this work, L was considered as the length of the coolant path inside the top reflector, D the hydraulic diameter, $\bar{V}$ the mean flow velocity and f the dimensionless Darcy friction factor, Eq. (9).

Considering that, in the HTR-10 at normal operations, the Reynolds number of the helium flow in the coolant channels is above 10 000 then the viscous effects can be neglected. In this Reynolds number range for the turbulent flow, the estimative of the Darcy friction factor f was calculated from the Colebrook–White correlation [24]:

$$\frac{1}{\sqrt{f}} = -2 * \log\left(\frac{\frac{e}{d_{2.5cm}}}{3.7} + \left(1 + \frac{2.51}{Re\sqrt{f}}\right)\right) \tag{9}$$

where e is roughness, and Re>4000.

2.7 Mesh Independence Study

A combination of tetrahedral and hexahedral elements in the flow domain and prism elements close to walls was used. The mesh generating software ANSYS Meshing was chosen to generate the meshes. In all of cases were ensure a y+ < 50 considering the $\kappa-\varepsilon$ turbulent model and scalable wall function. Also, in areas where local details were needed, the local mesh refinement was used to capture fine geometrical details. Additionally, it was checked that parameters like orthogonal quality, expansion factor and aspect ratio are within the recommended values [18]. A good mesh quality is essential for performing a good CFD analysis but it's not enough [18]. A preliminary analysis of the results is required to reach a mesh-independent solution and eliminate the false information induced by numerical reasons, e.g., computational geometry (mesh size – number of elements, etc.) and numerical scheme applied [25]. In this sense, a mesh sensitivity study was performed to analyze the suitability of the mesh.

In all prototypes, four different meshes (design points) with increasing mesh densities were analyzed. For this mesh sensitivity study, it is necessary to select the key parameters to be analyzed. Since the aim of this paper is to identify and characterize the impact on the main thermohydraulic parameters due to the approximation used to represent the coolant entry pattern into the core of the pebble bed high-temperature reactor prototypes, the mesh sensitivity study analyzed the average and maximum coolant temperature, as well as the average velocity inside the hot core zone.
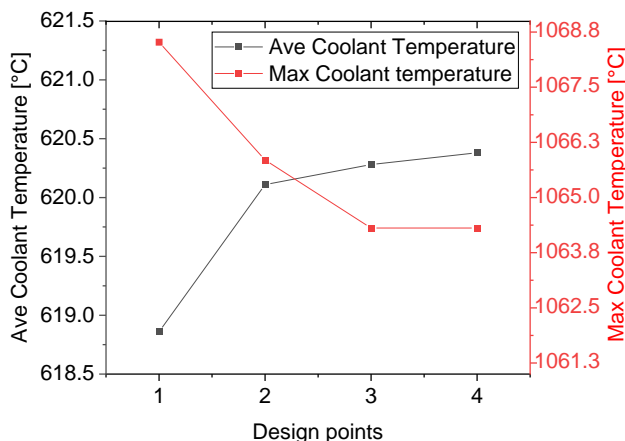
Figure 3. Coolant temperature inside the hot core zone for different meshes from Prototype 20x⌀12cm 30°

Also, the Grid Convergence Index (GCI) value, proposed by Roache in 1998 [26], was considered, which corresponds to the numerical uncertainty. In this case, the minimum numerical error considered was less than 1%. The Figure 3 and Figure 4 show the control parameters from four meshes with 0.6, 1.5, 4.3, and 7.6 million elements respectively.
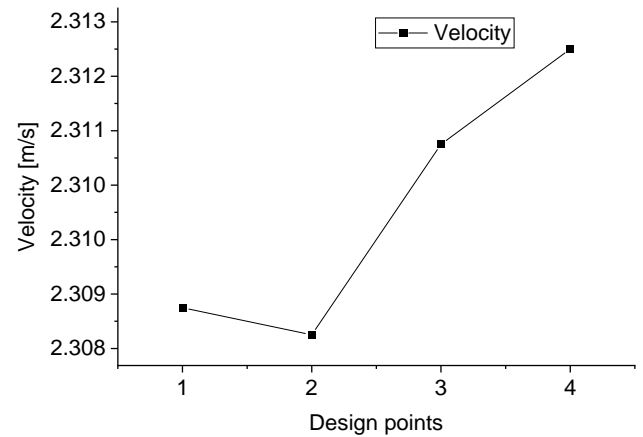
Figure 4. Velocity inside the hot core zone for different meshes from Prototype 20x⌀12cm 30°.

Figure 4 shows the average velocity values for the four different meshes for the Prototype 20x⌀12cm 30°. The four design points have a relative difference of less than 1% in all analyzed parameters for this entry pattern. These results show that there are no significant differences between them among the studied meshes. The same behavior was observed in the other prototypes.

As it is known that, the meshes with the least number of elements are the meshes that have the least computational requirements, then the meshes with the least number of elements were selected for the studies to be carried out. The Table 1 shows the properties and quality of the selected meshes. Is important to note that the analyzed prototypes of 20x⌀12cm have a similar mesh quantity to the simplified porous media model with around 1 million elements.

2.8 Computational Resources and Convergence

The time needed to converge a complex CFD analysis is more complicated than only considering the number of cores available and the mesh size. Other aspects of the hardware, such as memory, storage and interconnect speed will also make a difference, as will the specific choice of code and the temporal and spatial characteristics of the phenomena within the solution. All calculations were performed considering an RMS residual of 1E-05, which is typically sufficient for the majority of engineering applications. The Table 2 summarizes the computational resources needed for the solution of the five models.

Table 1. Properties of the selected meshes.

Selected Design Point	Prototype 460x⌀2.5cm 0°	Prototype 460x⌀2.5cm 30°	Prototype 20x⌀12cm 0°	Prototype 20x⌀12cm 30°	Simplified porous media model
Nodes 10^6	1.88	2.65	0.35	0.38	0.59
Elements 10^6	5.10	5.54	0.63	0.62	1.06
Aspect Ratio	53.00	54.00	40.00	15.00	82.00
Orth. Quality	32.60	32.50	27.40	32.70	31.60
Expansion Fact.	247.00	52.00	239.00	189.00	87.00

Table 2. Computational resources.

Model	Core	Memory [MBytes]	CPU time [s]	Iteration
Prototype 460x⌀2.5cm 0°	32	10149.29	1.339E+04	294
Prototype 460x⌀2.5cm 30°	32	9289.69	2.825E+04	600
Prototype 20x⌀12cm 0°	16	3273.12	9.257E+03	337
Prototype 20x⌀12cm 30°	16	3326.18	1.972E+03	448
Simplified porous media model	16	4043.77	6.912E+03	233

3. Results and Discussion

The ensuing section, delves into a qualitative examination aimed at identifying and characterizing the impact that the coolant entry pattern into the reactor core, on key thermohydraulic parameters within the reactor core. Specifically, our focus will be on comprehensively discussing the behavior of coolant velocity, pressure drops, and the temperatures of both the coolant and the fuel elements.

3.1 Velocity Discussion

The first thermohydraulic parameter to analyze is the coolant velocity. Following Figure 5, the depiction of the helium velocity profile before and after crossing the top reflector region is shown.

The colorimetric scale of Figure 5 a) was set from 0 to 10 m/s with the aim of highlighting, with greater contrast, the different flow regions, especially the coolant entry region into the reactor core. However, the maximum velocity reached at the top of the coolant channels was approximately 17 m/s in the five analyzed cases. As shown in Figure 5 a), the coolant rises through the ducts inside the reflectors and carbon bricks up to the cold plenum. Then, the coolant crosses the top reflector on its way up to the top core cavity using one of the five proposed models.

Figure 5 b) to f) show the flow distribution at this crossing for the five analyzed cases. In the prototype models with channels of 460x⌀2.5cm, the formation of small jets of coolant is observed. Those jets penetrate a small portion of the upper cavity of the core. The development of these small jets of coolant does not reach the bed of fuel elements, they diffuse before reaching the pebble-bed. On the other hand,
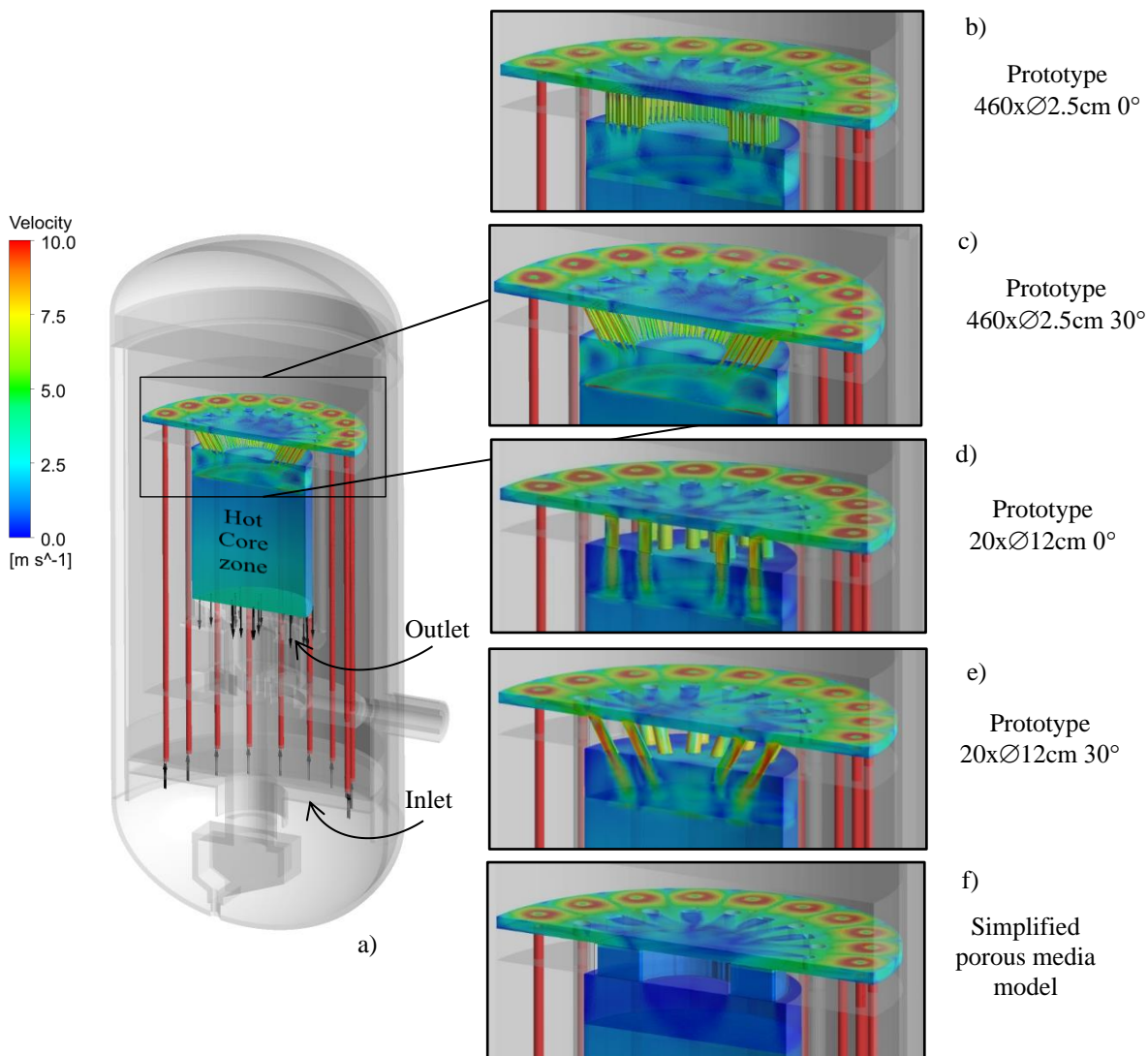

Figure 5. Modeled Coolant region inside the HTR-10 a), and the 3D volumetric representation of the velocity distribution profiles for the five computational models b) to f).

the jets of coolant in the prototypes of 20x∅12cm develop as they pass through the core cavity, indicating a lower impact of the diffusive effects. In the simplified porous media model, the formation of jets is not observed.
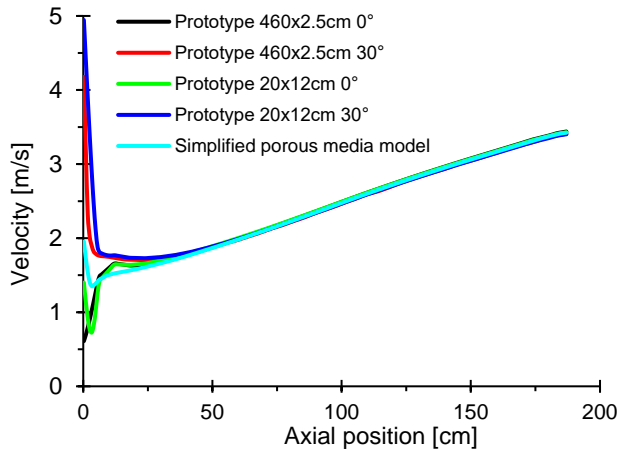

Figure 6. Velocity profiles at the center line of the reactor core.

After the coolant crosses the top cavity, the five schemes show a similar tendency. As expected, the coolant increases its speed as it passes through the core of fuel elements. Figure 6 display a linear increase in velocity from 1.78m/s at the beginning to 3.42m/s at the end of the pebble bed. This effect is due to the fact that when it crosses the fuel elements, the coolant is heated and its viscosity decreases. It is known that this reactor can increase its temperature by up to 3 times (250 °C - 950 °C) in normal operation.

Figure 7 shows using a colorimetric scale ranging from blue to white, the velocity profile at different distances of penetration of the coolant in the reactor core (0cm, 80cm and 170cm), for the five computational models studied. It is shown that at the beginning of the fuel elements (position, 0 cm) the coolant arrives with different patterns in each case. However, this difference disappears when entering the pebble bed (positions 80cm and 170cm). On the other hand, if the velocity profiles are represented in the radial positions at different depths, as shown in Figure 8, it is possible to notice that at 80cm and 170cm penetration the 5 models present practically the same prediction.

Performing a detailed analysis of the radial velocity distribution, it can be concluded that, for 50cm of penetration of the coolant in the fuel element bed, there is still a difference between the models (see Figure 7). This relative difference concerning to the average of the five computational models is small and can reach up to 6% at 50cm.

In summary, even though the analyzed models have different coolant distribution patterns at the beginning of the pebble of the fuel elements, these differences have a small impact on the prediction of the fluid movement inside the pebble. The estimated mean velocity coolant inside the pebble bed core was approximately 2.30 m/s, as shown in Figure 8 and Figure 9.

These results contribute valuable insights into the dynamic behavior of the coolant, aiding in the evaluation and enhancement of the reactor's design for optimal thermohydraulic efficiency.
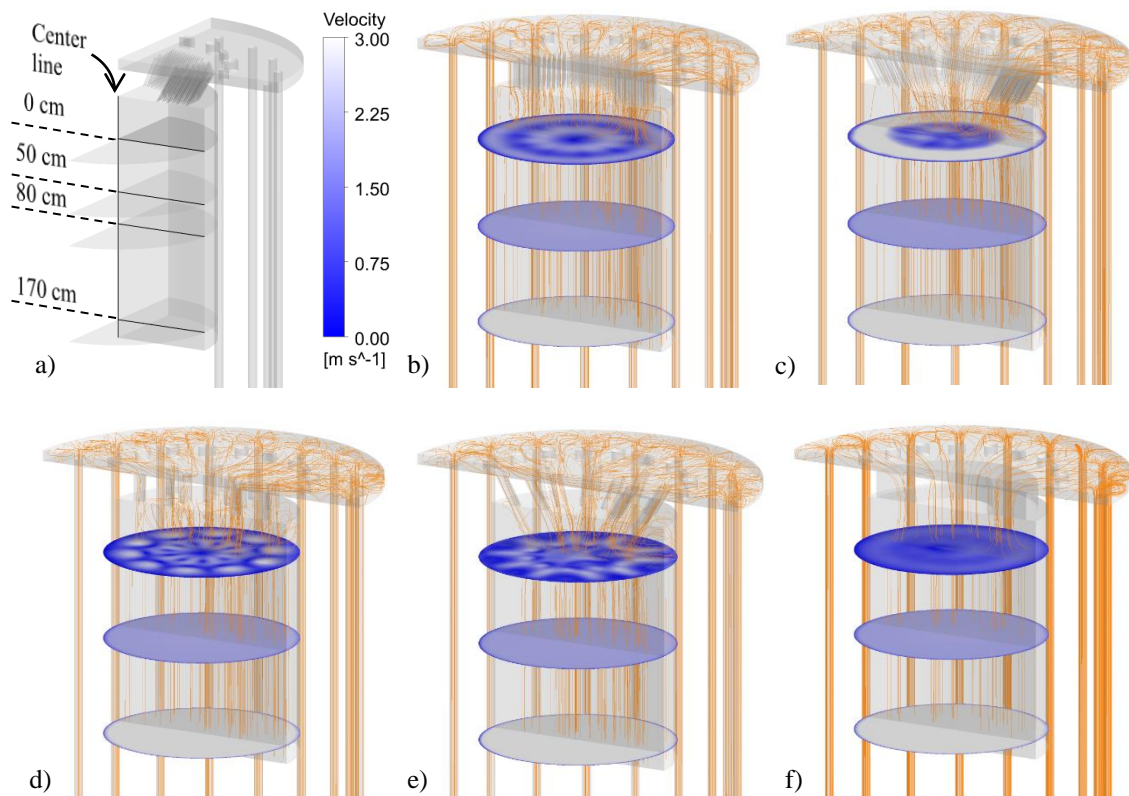

Figure 7. Velocity profiles at different penetration distances of the coolant in the reactor core: a) position lines, b) Prototype 460x∅2.5cm 0°, c) Prototype 460x∅2.5cm 30°, d) Prototype 20x∅12cm 0°, e) Prototype 20x∅12cm 30°, f) Simplified porous media model.
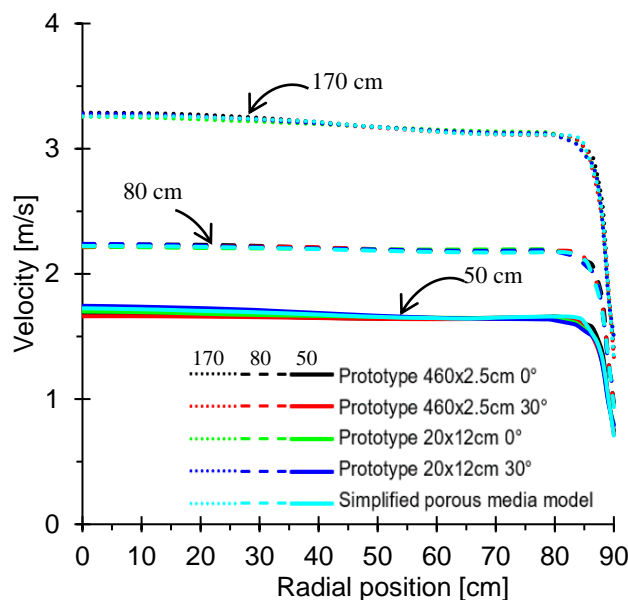
Figure 8. Radial velocity at three different heights, 50cm, 80cm and 170cm from the beginning of the pebble fuel elements.
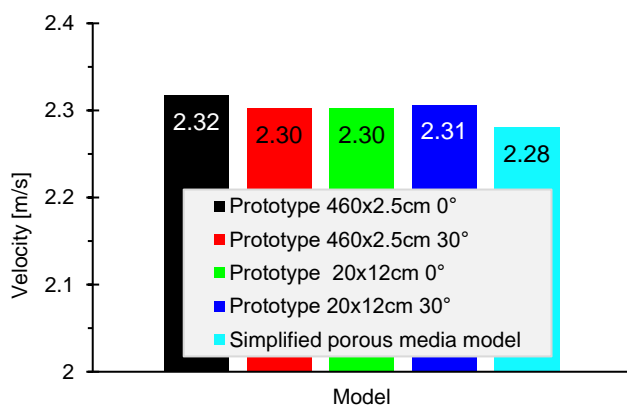

Figure 9. Average velocity in the Hot Core Zone.

3.2 Coolant and Fuel Elements Temperatures

The second thermohydraulic parameter to analyze was the coolant and fuel temperature. It is known that the highest temperatures are reached inside the fuel elements, which is where the heat by nuclear fission and radioactive decay is generated. After the heat is generated by nuclear fission inside the fuel elements, it heat is conducted to the external fuel surface. In general, for the extraction of this heat, the coolant and the structural elements act by convection, conduction, and radiation actively. Once the coolant is heated, this heat is conducted towards the steam generator. According to [12], [14], it is estimated that the highest temperatures in this reactor are found in the lower central region of the core. Therefore, with the interest of studying the behavior of the maximum temperatures in the coolant inside the reactor, the temperature in the center line will be analyzed.

Figure 10 shows the coolant temperature in the centerline of the hot core zone. From this figure, it can be identified that the five computational models present the same increasing trend of the fuel elements temperature. The heating occurs from a value close to the coolant at the inlet of the pebble bed until reaching the maximum temperature in the lower central

region of the core as seen in Figure 9. Also, it can be appreciated in Figure 9, that after reaching a depth of 180cm, the temperature of the coolant stops increasing. This is due to the used model of heat generation, having a drastic decrease in the power density for the last 7cm of the approximate active core, according to [14]. In this way, the last 7cm of the curves coincide with the region where the temperature stops increasing.

The highest temperature was obtained from the model of the Prototype 460x2.5cm 0°, which is the most conservative pattern from the point of view of safety. On the other hand, the model with the Prototype 20x12cm 30°, presents the least conservative tendency to estimate the highest temperature.
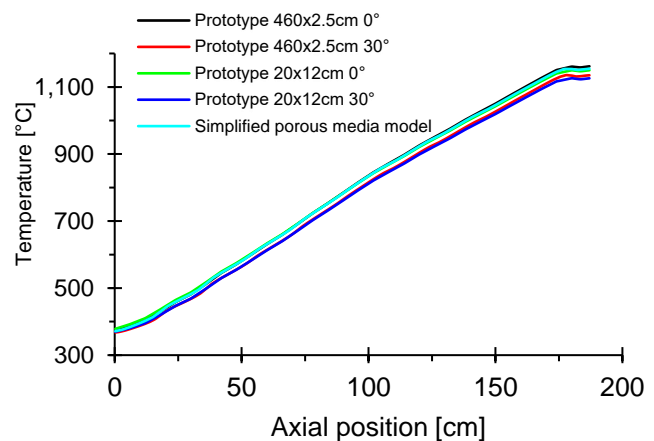

Figure 10. Coolant temperature in the centerline of the hot core zone.

The largest maximum relative difference between these two models was 35.7 °C, which represents approximately 3%. In summary, no significant differences were found in the estimated mean and maximum temperatures among the five computational models analyzed. It is important to note that this analysis is only qualitative since the objective of the article is to identify and characterize the impact of the coolant entry pattern into the reactor core on the main thermohydraulic parameters. For this reason, and with the aim of reducing the computational cost, adiabatic boundary conditions were considered in all surfaces as was indicated in the section 2.2. Thereby, estimated temperatures in all computational models were higher than those predicted by [12], [14]. In general, the values of the maximum temperatures in the normal operation in this reactor are lower. According to the [14] the fuel elements temperature must never exceed 1200 °C, which is the design limit temperature for the fuel elements.

In summary, the average and maximum estimated temperatures by the five models are shown in Table 3. From the analysis of the values shown in Table 3, it is concluded that the five models estimate the average values without significant differences. In the case of the maximum values, the Prototype of 460x2.5cm 0° estimates the highest values, both for the temperature of the coolant and the temperature on the surface of the fuel elements. The lowest maximum coolant temperature among the five models was obtained by the Prototype of 460x2.5cm 30° and the lowest fuel element surface temperature was obtained by the Prototype of 20x12cm 30°. The relative differences with respect to the mean value of the five models are less than 2%.

Table 3. Main temperatures in the hot core zone

| Model | Temperature [C] | | | | | | | |
| | Coolant in the core zone | | | | Fuel elements Surface | | | |
	Ave.	Max.	Mean	Dif.	Ave.	Max.	Mean	Dif.
Prototype 460x∅2.5cm 0°	618.05	1104.75		0.9%	724.24	1161.70		1.4%
Prototype 460x∅2.5cm 30°	617.94	1080.38		1.3%	723.98	1135.50		0.9%
Prototype 20x∅12cm 0°	618.44	1092.85	1095	0.2%	724.55	1149.95	1145	0.4%
Prototype 20x∅12cm 30°	619.26	1098.45		0.3%	725.29	1125.99		1.7%
Simplified porous media model	618.04	1099.75		0.3%	724.24	1155.88		0.9%

3.3 Pressure Drop

The last thermodynamic parameter to analyze is the pressure in the five computational models. In general, the steady-state simulation was performed at the nominal pressure of 3MPa as indicated [14]. This pressure is less than the safety limit (3.3MPa) approved by the China National Nuclear Safety Authority (NNSA) as operation limit to ensure the system and components safety [27].

The estimated pressure drop in the pebble bed was in agreement with the equations model discussed in [12]. In all the cases, the coolant pressure drops slightly till reaching the top helium plenum, then continues decreasing along the path inside the top reflector. Subsequently, a more pronounced pressure drop was observed as the coolant passed through the pebble bed. Similar behavior was reported in [12].
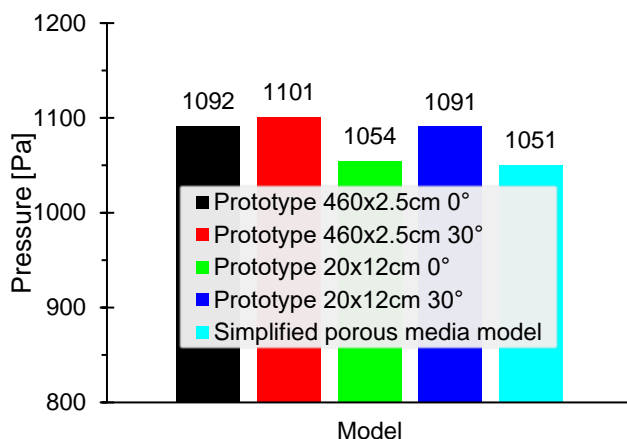

Figure 11. Total pressure drop in the five computational models.

The total pressure drop in the five computational models was shown in Figure 11. The five computational models show a similar total pressure drop, of approximately 1078 Pa.

Figure 12 shows the behavior of the pressure drop along the axial axis in the reactor core center line. As observed, the pressure remains approximately constant above 600 Pa in the region before the pebble bed entry. After the coolant enters the pebble bed, the pressure drops across the pebbles until the cone region. As observed for the temperature behavior, the entry pattern only has a small impact at the beginning of the pebble-bed modeling. In the first 25 cm of the top of the pebble-bed, this difference reaches less than 1% of the mean value between them.

4. Conclusions

This paper is part of the ongoing efforts to contribute to the prediction of the thermohydraulic behavior of one of the most promising Generation IV systems, the Very High
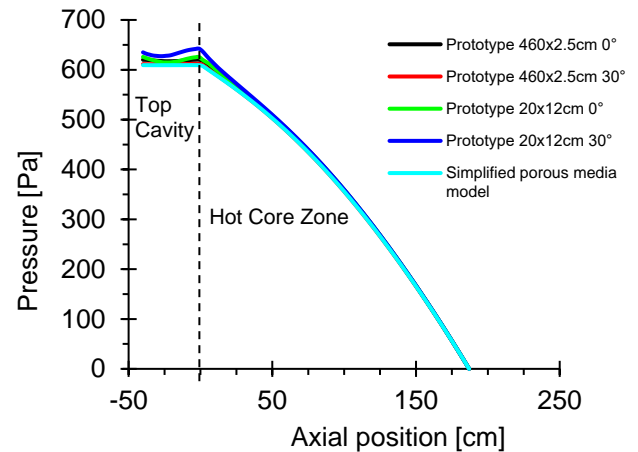

Figure 12. Pressure drop in the reactor core centerline.

Temperature gas-cooled Reactor, using three-dimensional modeling. For this purpose, this paper addresses one of the great challenges of nuclear thermohydraulic, which is the detailed full-scale modeling of complex structures. In this study, a comparison between five alternatives to represent the top reflector internal structures in a high temperature pebble bed SMR was developed. The primary objective of this study was to identify and characterize the influence of the coolant entry pattern into the reactor core on key thermohydraulic parameters. 460x2.5cm

From the analysis of the velocity profiles, it was found that the five models provoke different patterns of coolant distribution in the upper cavity of the reactor core. It was observed that the coolant entry patterns generated from the 460x2.5cm prototypes spread small jets and then diffuse quickly without penetrating the fuel element bed. On the other hand, the 20x12cm prototypes generate jets that reach the vicinity of the fuel element bed. The main difference was found in the distribution of coolant at the beginning of the bed of fuel elements, which quickly disappears. This difference between the 5 models is less than 6% in the first 10 cm of penetration in the pebble bed. The five inlet patterns maintain the same coolant distribution throughout virtually the entire fuel element bed. The temperature analysis revealed that all five models exhibit a consistent rate of temperature increase as they pass through the fuel elements. The greatest difference was evidenced between the model corresponding to the prototype 460x2.5cm 0° and 20x12cm 30°, being only 35.7 °C. The model that presents the highest values, therefore more conservative, is the prototype model of 460x2.5cm 30°. On the other hand, the lowest temperatures were obtained at 20x12cm 30°. The relative differences to the mean value of the five models are less than 2%. All five computational models exhibit a comparable total pressure drop, averaging around 1078 Pa. As observed for the temperature behavior, the entry pattern only has a small impact at the beginning of the pebble-bed modeling.

In the first 25cm of the top of the pebble-bed, this difference reaches less than 1% of the mean value between them.

Explicitly, it was demonstrated that even though the analyzed models exhibit distinct coolant distribution patterns at the initial stage of the pebble bed of fuel elements, these variations have a minimal impact on predicting the global temperatures and fluid movement inside the pebble. This distinct lack of differences in the overall results of the main parameters of interest, regardless of the entry pattern model used, might justify why, despite the reactor operators not sharing specific details about the top reflector internal structure, researchers have conducted successful simulation of the HTR-10 reactor over the years.

This conclusion is reinforced as even the porous media model shows a strong correlation with the prototype models concerning the maximum fuel temperature, average fuel temperature, and helium velocity. The prediction of the pressure drop from the Darcy-Weisbach approach is an acceptable prediction as well. In this study, the potential applicability of the porous media models for an integral full-scale reactor simulation in the future was demonstrated. As a benefit, the porous media model as well the simplified models reduces the mesh quantity from a detailed prototypic model. Correspondingly, the computation time was reduced.

Nomenclature

SMR	Small Modular Reactors
AVR	German: Arbeitsgemeinschaft Versuchsreaktor
CAD	Computer Aided Design
CFD	Computational Fluid Dynamics
DNS	Direct Numerical Simulation
GIF	Generation IV International Forum
HTGR	High-Temperature Gas-Cooled Reactors
HTR	High Temperature Reactor
HTTR	High-Temperature Test Reactor
IAEA	International Atomic Energy Agency
KTA	German: Kerntechnischer Ausschuss
LOCA	Loss-of-Coolant Accident
NNSA	China National Nuclear Safety Authority
RANS	Reynolds Averaged Navier-Stokes
RCFR	Rated Coolant Flow Rate
RPV	Reactor Pressure Vessel
RSM	Root Mean Square
THTR	Thorium High-Temperature Reactor
VHTR	Very-High-Temperature Reactor
ρ	density $[kg/m^3]$
τ	stress tensor $[Pa]$
t	time $[s]$
λ	thermal conductivity $[W/mK]$
μ	dynamic viscosity $[Pa\ s]$
U	velocity $[m/s]$
p	pressure $[Pa]$
S_M	momentum source $[kg\ m/s]$
h	enthalpy $[J]$
T	temperature $[K]$
S_E	heat source $[W]$
C_p	specific heat capacity at constant pressure $[J/kg\ K]$
L	length of the coolant path inside the top reflector $[m]$
f	Darcy friction factor
$\bar{V}$	mean flow velocity
D	hydraulic diameter $[m]$
e	roughness
Re	Reynolds Number
$\dot{m}_{2.5cm}$	mass flow rate crossing an individual channel $[kg/s]$
$d_{2.5cm}$	diameter of a channel $[m]$
$A_{2.5cm}$	cross section area of a channel $[m^2]$

References:

[1] OECD/NEA, "Advanced Nuclear Reactor Systems and Future Energy Market Needs," 2021.

[2] IEA, "World Energy Outlook 2021," Paris, 2021.

[3] OECD/NEA, "Generation IV International Forum, Technology Roadmap Update for Generation IV Nuclear Energy Systems," Paris, 2014.

[4] IAEA, "Guidance on Nuclear Energy Cogeneration," Vienna, 2019.

[5] GIF, "GIF R&D Outlook for Generation IV Nuclear Energy Systems: 2018 Update," 2018.

[6] B. Zohuri, "Generation IV nuclear reactors," in *Nuclear Reactor Technology Development and Utilization*, A. N. Salah Ud-Din Khan, Ed., Elsevier, 2020, pp. 213–246. doi: 10.1016/B978-0-12-818483-7.00006-8.

[7] IAEA, "Nuclear Power Reactors in the World," 2021.

[8] GIF, "Generation IV International Forum 2020 Annual Report," 2020.

[9] GIF/RSWG, "Basis for the Safety Approach for Design & Assessment of Generation IV Nuclear Systems," Vienna, 2021.

[10] D. E. Shropshire, A. Foss, and E. Kurt, "Advanced Nuclear Technology Cost Reduction Strategies and Systematic Economic Review," 2021.

[11] Y. A. Hassan and H. Students, "Theoretical Foundations and Applications of Computational Fluid Dynamics in Nuclear Engineering," Trieste, 2022.

[12] A. Gámez Rodríguez, L. Y. Rojas Mazaira, C. R. García Hernández, D. Dominguez Sanchez, and C. A. Brayner Oliveira Lira, "An integral 3D full-scale steady-state thermohydraulic calculation of the high temperature pebble bed gas-cooled reactor HTR-10," *Nucl. Eng. Des.*, vol. 373, no. December 2020, 2021, doi: 10.1016/j.nucengdes.2020.111011.

[13] C. Wang, Y. Liu, X. Sun, and P. Sabharwall, "A hybrid porous model for full reactor core scale CFD investigation of a prismatic HTGR," *Ann. Nucl. Energy*, vol. 151, p. 107916, 2021, doi: 10.1016/j.anucene.2020.107916.

[14] IAEA, "Evaluation of High Temperature Gas Cooled Reactor Performance: Benchmark Analysis Related to the PBMR-400, PBMM, GT-MHR, HTR-10 and the ASTRA Critical Facility," IAEA, Vienna, 2013.

[15] Z. Zhang, J. Liu, S. He, Z. Zhang, and S. Yu, "Structural design of ceramic internals of HTR-10," *Nucl. Eng. Des.*, vol. 218, no. 1–3, pp. 123–136, 2002, doi: 10.1016/S0029-5493(02)00205-4.

[16] Y. M. Ferng and C. T. Chen, "CFD investigating

thermal-hydraulic characteristics and hydrogen generation from graphite-water reaction after SG tube rupture in HTR-10 reactor," *Appl. Therm. Eng.*, vol. 31, no. 14–15, pp. 2430–2438, 2011, doi: 10.1016/j.applthermaleng.2011.04.007.

[17] Y. M. Ferng and C. W. Chi, "CFD investigating the air ingress accident for a HTGR simulation of graphite corrosion oxidation," *Nucl. Eng. Des.*, vol. 248, pp. 55–65, 2012, doi: 10.1016/j.nucengdes.2012.03.041.

[18] I. ANSYS, *ANSYS CFX Solver Modeling Guide*, 19.0. Canonsburg, PA, 2018.

[19] D. Milian Pérez, A. Gámez Rodríguez, L. Hernández Pardo, M. L. Daniel Evelio, and B. de O. L. Carlos Albrto, "Implementation of a Multi-cell Approach in the Multi-Physics Calculations of an Aqueous Homogeneous Reactor," *Int. J. Thermodyn.*, vol. 24, no. 4, pp. 125–133, 2021, doi: 10.5541/ijot.895287.

[20] I. ANSYS, *ANSYS CFX-Solver Theory Guide*, 19.0. Canonsburg, PA, 2018.

[21] KTA, "Reactor Core Design of High-Temperature Gas-Cooled Reactors Part 2: Heat Transfer in Spherical Fuel Elements," KTA, 1983.

[22] KTA, "Reactor Core Design for High-Temperature Gas-Cooled Reactor Part 1: Calculation of the Material Properties of Helium," KTA, 1978.

[23] Z. Gao and L. Shi, "Thermal hydraulic calculation of the HTR-10 for the initial and equilibrium core," *Nucl. Eng. Des.*, vol. 218, no. 1–3, pp. 51–64, 2002, doi: 10.1016/S0029-5493(02)00198-X.

[24] J. C. L. Pritchard, J. Philip, *Introduction to Fluid Mechanics*, 8th ed. John Wiley & Sons, Inc, 2011.

[25] H. Wang and Z. J. Zhai, "Analyzing grid independency and numerical viscosity of computational fluid dynamics for indoor environment applications," *Build. Environ.*, vol. 52, pp. 107–118, 2012, doi: 10.1016/j.buildenv.2011.12.019.

[26] P. J. Roache, *Verification and validation in computational science and engineering*. Albuquerque, N.M: Hermosa Publishers, 1998.

[27] S. Hu, R. Wang, and Z. Gao, "Safety demonstration tests on HTR-10," *2nd Int. Top. Meet. High Temp. React. Technol.*, pp. 22–24, 2004.